

Geophysical Research Letters[®]



RESEARCH LETTER

10.1029/2022GL101717

Variations of Carbonyl Sulfide During the Dry/Wet Seasons Over the Amazon

Xinyue Wang¹, Xun Jiang¹ , King-Fai Li² , Mao-Chang Liang³ , Le Kuai⁴ , Lin Tan², and Yuk L. Yung^{4,5}

¹Department of Earth and Atmospheric Sciences, University of Houston, Houston, TX, USA, ²Department of Environmental Sciences, University of California, Riverside, Riverside, CA, USA, ³Institute of Earth Sciences, Academia Sinica, Taipei, Taiwan, ⁴Jet Propulsion Laboratory, California Institute of Technology, Pasadena, CA, USA, ⁵Division of Geological and Planetary Sciences, California Institute of Technology, Pasadena, CA, USA

Key Points:

- Tropospheric Emission Spectrometer OCS concentrations are higher over the central and southern parts of the Amazon during the dry season than the wet season
- High OCS concentrations are related to reduced vegetation uptake, enhanced biomass burning, and increased sinking air
- MOZART-4 captures the observed positive OCS anomalies over the central and southern Amazon during August–October (dry season)

Supporting Information:

Supporting Information may be found in the online version of this article.

Correspondence to:

X. Jiang,
xjiang7@uh.edu

Citation:

Wang, X., Jiang, X., Li, K.-F., Liang, M.-C., Kuai, L., Tan, L., & Yung, Y. L. (2023). Variations of Carbonyl sulfide during the dry/wet seasons over the Amazon. *Geophysical Research Letters*, 50, e2022GL101717. <https://doi.org/10.1029/2022GL101717>

Received 13 OCT 2022

Accepted 5 FEB 2023

Author Contributions:

Conceptualization: Xinyue Wang, Xun Jiang

Data curation: Xinyue Wang, Lin Tan

Formal analysis: Xinyue Wang, Xun Jiang

Funding acquisition: Xun Jiang

Investigation: Xinyue Wang, Xun Jiang

Methodology: Xinyue Wang, Xun Jiang

Resources: Xinyue Wang

Software: Xinyue Wang

Supervision: Xun Jiang

Validation: Xinyue Wang

Visualization: Xinyue Wang

© 2023 The Authors.

This is an open access article under the terms of the [Creative Commons Attribution-NonCommercial License](https://creativecommons.org/licenses/by/4.0/), which permits use, distribution and reproduction in any medium, provided the original work is properly cited and is not used for commercial purposes.

Abstract Mid-tropospheric Carbonyl sulfide (OCS) retrievals from the Tropospheric Emission Spectrometer (TES) are utilized to study OCS distributions during the dry/wet seasons over the Amazon rainforest. TES OCS retrievals reveal positive OCS anomalies (~16 ppt) over the central and southern parts of the Amazon during August–October (dry season) compared to January–March (wet season). There is less OCS taken up by vegetation and soil and more OCS released from biomass burning during the dry season, which causes an increase in OCS concentrations. Strong sinking air during the dry season also helps to trap OCS and this contributes to positive OCS anomalies. MOZART-4 model captures positive OCS anomalies over the central and southern regions of the Amazon and negative OCS anomalies over the northern part of the Amazon, which are similar to those from TES mid-tropospheric OCS retrievals. Our studies can help us better understand OCS variations and photosynthetic activities.

Plain Language Summary As a photosynthetic tracer, OCS can help us better understand photosynthetic activities, the biosphere-atmosphere interaction, and the carbon sink. There are positive OCS anomalies (~16 ppt) over the central and southern parts of the Amazon during August–October (dry season), which is related to reduced OCS uptake from vegetation and soil, enhanced OCS emission from biomass burning, and strengthened sinking air. MOZART-4 is used to simulate the OCS variations during dry/wet seasons. Model results are similar to those from Tropospheric Emission Spectrometer OCS retrievals. However, there are some differences between the spatial distributions of OCS in the MOZART-4 model and the satellite retrievals. Results in this study can help us better understand the variability of OCS and photosynthetic activities over the Amazon rainforest, which is the biggest rainforest and one of the largest sinks of OCS.

1. Introduction

Carbonyl sulfide (OCS) is an important compound in the global sulfur cycle (e.g., Chin & Davis, 1995; Crutzen, 1976; Ko et al., 2003; Notholt et al., 2003). OCS can help to form atmospheric sulfate aerosols that plays an important role in the radiative energy budget and climate forcing (Crutzen, 1976). OCS can be released to the atmosphere directly from ocean and anthropogenic sources, and indirectly through the oxidation of dimethyl sulfide and carbon disulfide (Chin & Davis, 1993; Kettle et al., 2002; Watts, 2000).

OCS is removed from the atmosphere by vegetation uptake through hydrolysis during photosynthesis (Brown & Bell, 1986; Campbell et al., 2008; Kettle et al., 2002; Protoschill-Krebs & Kesselmeier, 1992; Protoschill-Krebs & Wilhelm, 1996). Since OCS is only related to photosynthesis processes, OCS can be used to monitor the photosynthetic activities (Berry et al., 2013; Hu et al., 2021; Maseyk et al., 2014; Spielmann et al., 2019). Kooijmans et al. (2021) have updated the Simple Biosphere Model version 4 (SiB4) and the improved biospheric and soil OCS fluxes agree well with observations from different biomes, agricultural fields, and fertilized grassland. In a different study, Maignan et al. (2021) used a mechanistic model to represent OCS vegetation uptake in the Organizing Carbon and Hydrology In Dynamic Ecosystems (ORCHIDEE) land-surface model and noticed that simulated OCS vegetation flux are similar to field observations at two stations although with a smaller daily amplitude. OCS can also be removed from the atmosphere by soil, photolysis, and the reaction with the hydroxyl radical (Chin & Davis, 1993; Kettle et al., 2002; Watts, 2000). Abadie et al. (2022) utilized a mechanistic soil

Writing – original draft: Xinyue Wang, Xun Jiang

Writing – review & editing: Xinyue Wang, Xun Jiang, King-Fai Li, Mao-Chang Liang, Le Kuai, Lin Tan, Yuk L. Yung

model in ORCHIDEE land-surface model to simulate OCS soil flux and noticed that the simulated OCS soil flux agrees reasonably well with observations at seven sites with an error of $\sim 1.6 \text{ pmol m}^{-2} \text{ s}^{-1}$.

It is known that the ocean is the major source of atmospheric OCS (Kettle et al., 2002; Montzka et al., 2007; Watts, 2000). Using numerical model for the ocean, Lennartz et al. (2021) estimated global OCS oceanic emissions and revealed that the highest concentrations of OCS oceanic emission are present in high-latitude cold waters and coast areas. In addition to ocean, anthropogenic activities and biomass burning are other important sources of atmospheric OCS (e.g., Blake et al., 2008; Campbell et al., 2015). Using new emission measurements and material-specific data, Campbell et al. (2015) developed a global anthropogenic OCS inventory for 1850–2013. In a following study, Zumkehr et al. (2018) estimated anthropogenic OCS source using emission factors and industry activity data in 1980–2012. For the OCS biomass burning emission, Stinecipher et al. (2019) recently proposed a latest OCS biomass burning emission with a global average annual flux of $60 \pm 37 \text{ Gg S yr}^{-1}$, which is consistent with observations.

Atmospheric OCS concentrations have been monitored at the surface and from air balloons, aircraft, and satellites. The NOAA-ESRL network provides long-term OCS data at 14 surface stations with most stations over North America (Montzka et al., 2007). OCS balloon measurements are available from New Mexico, Sweden, and Alaska (Krysztofiak et al., 2014). The HIAPER Pole-to-Pole Observations (HIPPO) flights provide aircraft OCS measurements over the ocean (Wofsy, 2011). Satellite OCS retrievals are available in the mid-troposphere from the Aura Tropospheric Emission Spectrometer (TES) (Kuai et al., 2014, 2015), in the upper troposphere and stratosphere from the Michelson Interferometer for Passive Atmospheric Sounding (Glatthor et al., 2015, 2017), and in the stratosphere from the Fourier Transform Spectrometer of the Atmospheric Chemistry Experiment (ACE-FTS) (Boone et al., 2005). Kuai et al. (2014) have retrieved OCS over ocean and found TES OCS retrievals are consistent with HIPPO aircraft measurements. To retrieve OCS over land, the algorithm needs to consider surface emissivity (Kuai et al., 2014, 2015). Since there is no field campaign OCS data over the Amazon, satellite OCS retrievals over the Amazon are extremely important to understand atmospheric OCS and OCS surface fluxes over the biggest rainforest.

Numerical models have been utilized to simulate OCS and better understand OCS surface flux. Using a global carbon cycle model (SiB3) and an atmospheric transport model, Berry et al. (2013) reproduced the OCS seasonal variations at 12 surface sites. Ma et al. (2021) conducted a global inverse modeling of OCS using the TM5-4DVAR chemistry-transport model and noticed that the assimilation of HIPPO observations improves model results. Remaud et al. (2022) assimilated OCS and CO_2 observations to atmospheric transport model and optimized biospheric OCS fluxes in the ORCHIDEE global land surface model. Ma et al. (2021) and Remaud et al. (2022) also identified missing OCS sources in the tropical regions, which might be related to the underestimated ocean emission, overestimated biosphere uptake, and biomass burning source in the tropics. To better understand the carbon uptake over the Amazon, Stinecipher et al. (2022) used GEOS-Chem to simulate OCS and further estimated Amazonian gross primary production (GPP) values. They found that the derived GPP values are consistent with TRENDY models and observations over the Amazon and the smaller plant sink can help to explain the missing OCS sources in the tropics (Stinecipher et al., 2022).

In this paper, we will focus on the mid-troposphere and utilize TES OCS retrievals to explore the impact of dry/wet conditions on mid-tropospheric OCS distributions over the Amazon basin, because the Amazon rainforest is one of largest sinks for OCS (e.g., Kettle et al., 2002). OCS retrievals from satellite-borne instruments can be used to investigate the photosynthetic activities over the biggest rain forest during the dry/wet seasons. Meteorological data (e.g., horizontal winds, vertical pressure velocity) will be used to test the impact of transport on the distribution of OCS. A chemistry-transport model will be used to investigate how surface sources and atmospheric processes affect the OCS variations in the atmosphere during different seasons. Results obtained from this study can improve our understanding of photosynthetic activities and the OCS variations over the Amazon basin.

2. Data and Model

2.1. OCS Retrievals From TES

Mid-tropospheric OCS retrieval from TES infrared spectral measurements (Kuai et al., 2014, 2015) are used in this paper. TES was a Fourier Transform Spectrometer measuring the radiance emitted from Earth. The TES OCS data are retrieved using radiance data from $2,034$ to $2,075 \text{ cm}^{-1}$ (Kuai et al., 2014; Rodgers, 2000), and have a

maximum sensitivity in the mid-troposphere (300–500 hPa). Monthly mean TES mid-tropospheric OCS retrievals are available from January 2006 to December 2011. The error for monthly mean TES OCS data is about 7 ppt (Kuai et al., 2014, 2015). The TES OCS data have been regridded to $4^\circ \times 5^\circ$ in latitude \times longitude.

2.2. Other Data

Meteorological data (zonal wind, meridional wind, vertical pressure velocity) at 511 hPa, and surface soil temperature from National Centers for Environmental Prediction Reanalysis 2 (NCEP2) (Kanamitsu et al., 2002) are used to explore the impact of meteorology on the distribution of OCS. Monthly means of these parameters are available from January 1979 to the present. The spatial resolution of 511 hPa zonal wind, meridional wind, and vertical pressure velocity is $2.5^\circ \times 2.5^\circ$ in latitude \times longitude, while the spatial resolution of surface soil temperature is $1.9^\circ \times 1.875^\circ$ in latitude \times longitude.

Precipitation data from the Global Precipitation Climatology Project (GPCP) (Adler et al., 2018) are used in this study to investigate the variations of precipitation during different seasons. GPCP Version 2.3 precipitation data are available from January 1979 to present, with a spatial resolution of $2.5^\circ \times 2.5^\circ$ in latitude \times longitude.

2.3. MOZART-4 Model

The Model for Ozone and Related Chemical Tracers, version 4 (MOZART-4) is used in this study to simulate OCS. Meteorological data used to drive MOZART-4 are the NCEP Reanalysis 1 data sets (Kalnay et al., 1996). The horizontal spatial resolution of MOZART-4 is $2.8^\circ \times 2.8^\circ$ in latitude \times longitude. There are 28 vertical layers covering from the surface to 45 km (Emmons et al., 2010). Climatological OCS surface emissions from vegetation, biomass burning, soil, anthropogenic sources, and the oceans are used as boundary conditions for the MOZART-4 model. The fluxes from vegetation and soil are from the SiB4 (Kooijmans et al., 2021). SiB4 incorporates plant phenology at different stages and photosynthetic activities at different seasons (Kooijmans et al., 2021). A mechanistic model is used in SiB4 to represent OCS soil uptake and production, which can better simulate OCS land flux over the agricultural regions (Kooijmans et al., 2021). OCS biomass burning emissions are derived from the global fire emission database, which are consistent with global atmospheric composition monitoring network observations (Stinecipher et al., 2019). OCS anthropogenic fluxes are taken from Campbell et al. (2015). Oceanic OCS emissions are estimated by a numerical model driven by ERA5 Reanalysis data and MODIS chromophoric dissolved organic matter (Lennartz et al., 2021), which agree well with observations. The MOZART-4 model is run over the global domain. The net global OCS budget is $\sim 0.2 \text{ Gg S yr}^{-1}$ ($<0.02\%$ of the total OCS sources/sinks), which means that the global OCS budget is balanced. The simulated tropospheric OCS is ~ 500 ppt in MOZART-4., which is consistent with results in previous studies (e.g., Chin & Davis, 1995; Glatthor et al., 2017; Kuai et al., 2014; Notholt et al., 2003; Remaud et al., 2022; Thornton et al., 1996; Whelan et al., 2018).

3. Results

January–March is the wet season and August–October is the dry season for the Amazon basin (e.g., Jiang et al., 2021). GPCP Version 2.3 precipitation averaged in January–March (wet season) and August–October (dry season) are shown in Figure S1 in Supporting Information S1. Over the Amazon, the mean precipitation is about $250 \text{ mm month}^{-1}$ (January–March; wet; Figure S1a in Supporting Information S1) and 90 mm month^{-1} (August–October, dry; Figure S1b in Supporting Information S1), respectively. The Inter-Tropical Convergence Zone is over the Amazon basin during January–March (wet season) and over the northern part of the Amazon during August–October (dry season). As a result, there is less precipitation over most regions of the Amazon during August–October, while there is more precipitation over the northern part of the Amazon during August–October (Figure S1b in Supporting Information S1). Differences in the precipitation between two seasons (dry—wet) are shown in Figure S1c in Supporting Information S1. The Central and Southern Amazon region received significantly less precipitation during the dry season (August–October) than the wet season (January–March).

TES mid-tropospheric OCS, which has a maximum sensitivity at 511 hPa, was investigated during January–March (wet season) and August–October (dry season) over the Amazon. The results are shown in Figure 1. During January–March (wet season), more precipitation is associated with more photosynthesis over the Amazon basin (e.g., Albright et al., 2022). Since OCS is absorbed by vegetation during photosynthesis, OCS concentrations are relatively low over the Amazon basin during January–March (wet season) (Figure 1a). During August–October (dry season), less precipitation is associated with less photosynthesis. As a result, the OCS

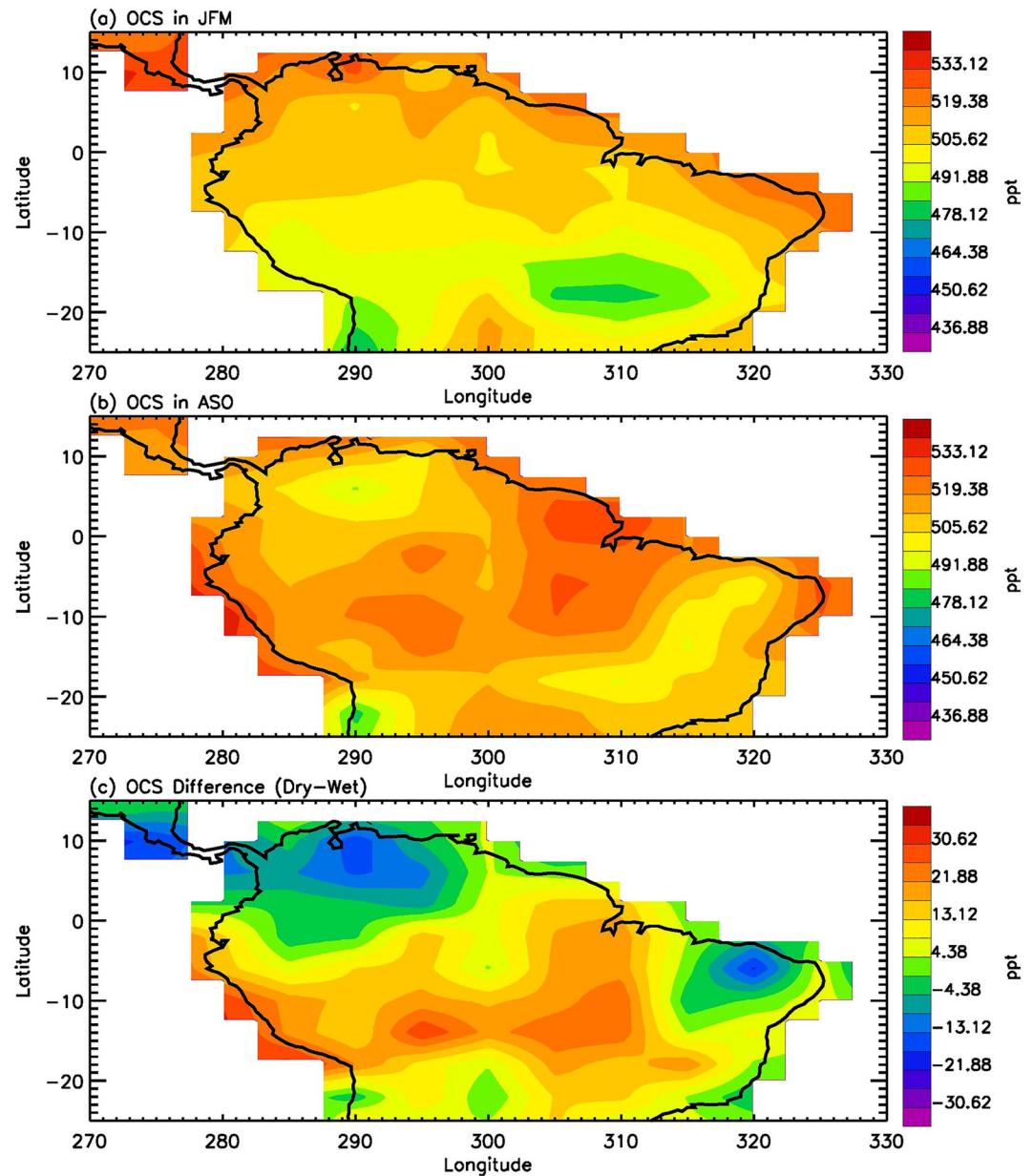


Figure 1. (a) Tropospheric Emission Spectrometer (TES) mid-tropospheric OCS averaged for January–March, 2006–2011 (wet season). (b) TES mid-tropospheric OCS averaged for August–October, 2006–2011 (dry season). (c) TES mid-tropospheric OCS difference between two seasons (dry and wet). Units are ppt.

concentrations are higher over the Amazon basin during August–October (dry season) (Figure 1b). Differences in TES mid-tropospheric OCS between August–October (dry season) and January–March (wet season) are shown in Figure 1c. There is more OCS (~16 ppt) over the Amazon basin as a result of low photosynthetic activities during August–October (dry season). There are negative OCS anomalies over the eastern Amazon and northern part of Amazon, which is consistent with positive precipitation anomalies over those regions (Figure S1c in Supporting Information S1). There are ~160 TES OCS retrievals (with good quality) in each grid cell for each of the dry and wet seasons. The OCS error in each grid cell is equal to the OCS standard deviation (~7 ppt) divided by the square root of number of data points (Albright et al., 2022; Bevington & Robinson, 2003). As a result, the OCS error is <0.6 ppt in each grid cell, which is much smaller than the 16 ppt OCS difference shown in Figure 1c.

To determine the influence of meteorological fields on the distribution of TES mid-tropospheric OCS at 511 hPa, we compared the vertical pressure velocity and horizontal winds at this altitude during January–March (wet

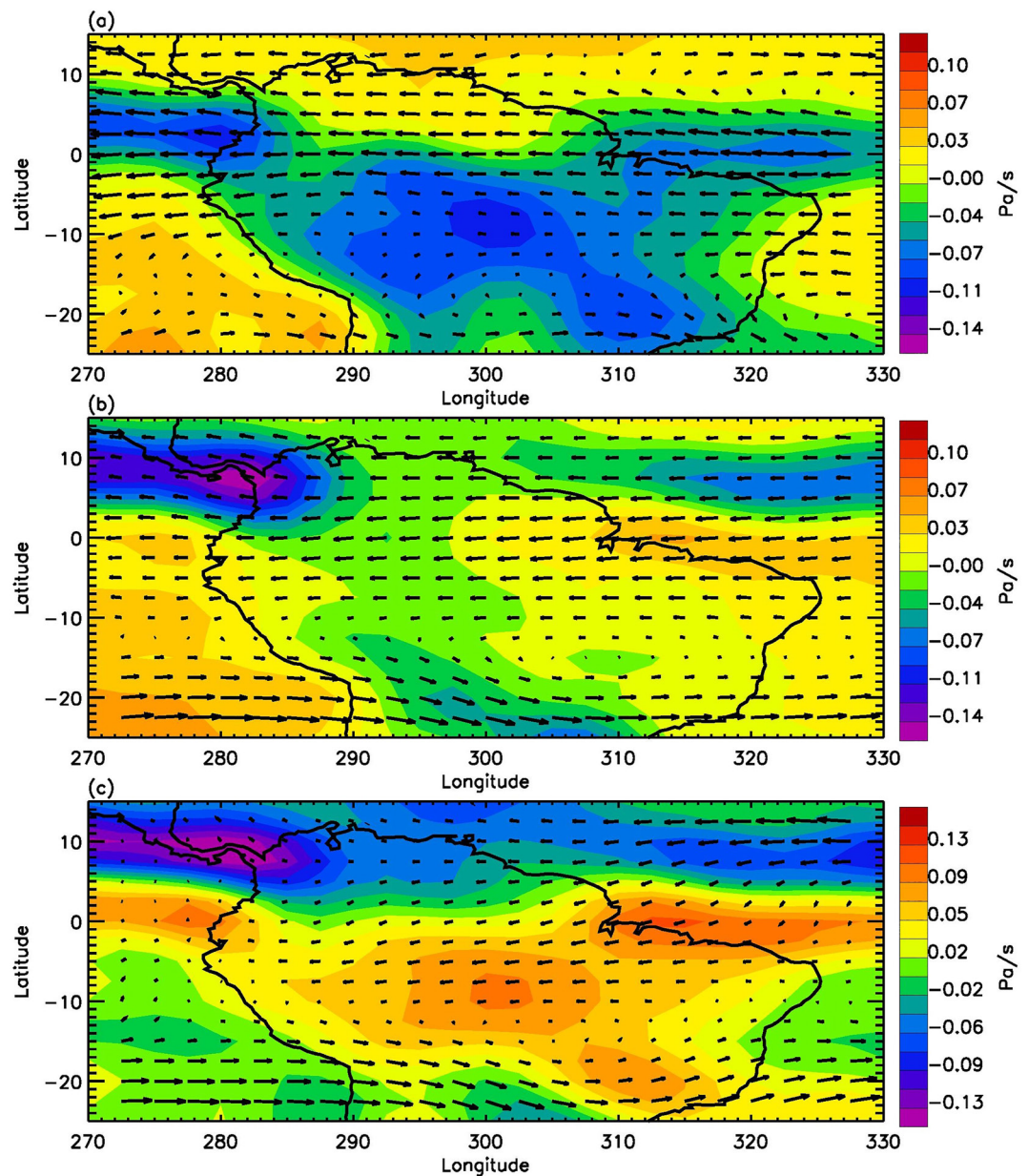


Figure 2. (a) National Centers for Environmental Prediction Reanalysis 2 (NCEP2) 511 hPa vertical pressure velocity and horizontal winds averaged for January–March, 2006–2011 (wet season). (b) NCEP2 511 hPa vertical pressure velocity and horizontal winds averaged for August–October, 2006–2011 (dry season). (c) NCEP2 511 hPa vertical pressure velocity and horizontal winds difference between two seasons (dry and wet). Units for the vertical pressure velocity is Pa s^{-1} .

season) and August–October (dry season) in Figure 2. NCEP2 vertical pressure velocity and horizontal winds were interpolated to 511 hPa. During January–March (wet season), there is a large negative vertical pressure velocity anomaly over the Amazon basin (Figure 2a), which indicates rising air over the basin. During August–October (dry season), there are regions with positive vertical pressure velocity (sinking air) over the eastern and western part of the Amazon basin (Figure 2b). Differences in vertical pressure velocity between August–October (dry) and January–March (wet) seasons are shown in Figure 2c. Positive vertical pressure velocity anomalies dominate the Amazon basin during August–October (dry season) relative to January–March (wet season), which suggests less rising air (or more sinking air) over the basin during August–October (dry season). The sinking air can help to trap OCS over the basin and contribute to positive OCS anomalies over the Amazon basin (Figure 1c). There are easterly winds at the Northern and Central Amazon and westerly winds at the southern Amazon for

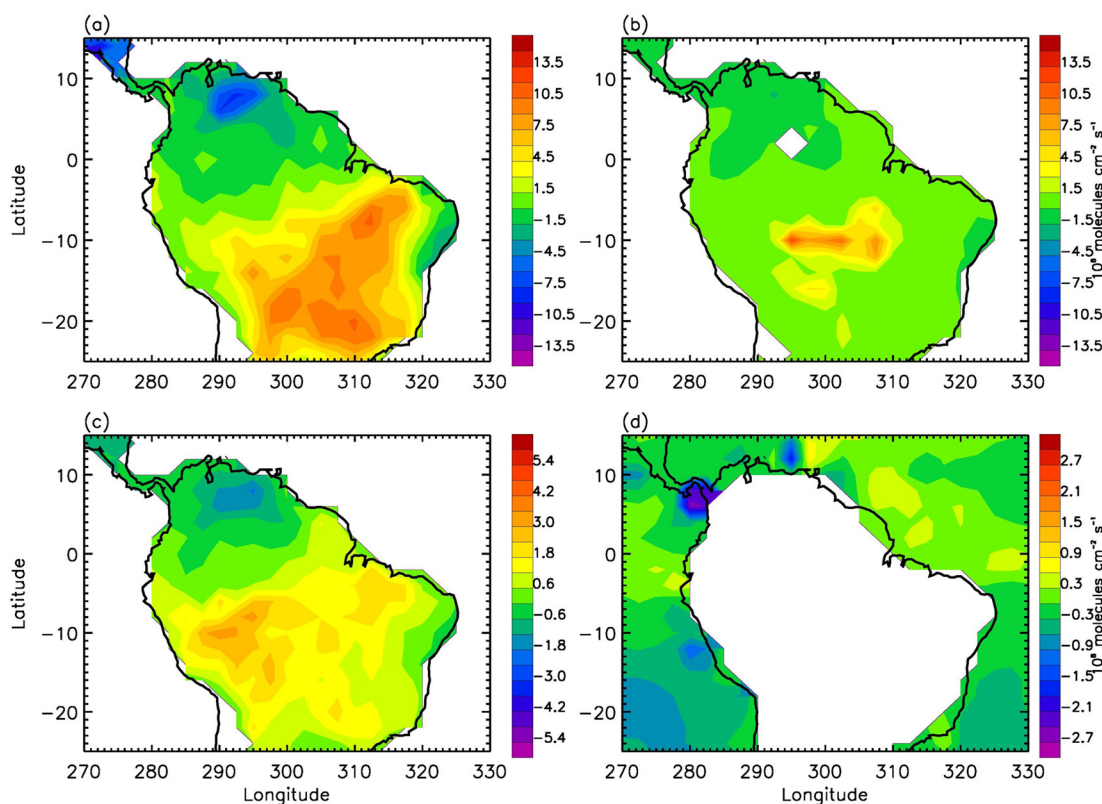


Figure 3. MOZART-4 OCS surface emission differences between two seasons (dry and wet) (a) OCS emission from the plant uptake, (b) OCS emission from the biomass burning, (c) OCS emission from the soil, and (d) OCS emission from the ocean. Units are 10^8 molecules $\text{cm}^{-2} \text{s}^{-1}$.

both seasons. Horizontal wind differences (dry season—wet season) demonstrate easterly wind anomalies in the central and northern part of Amazon and westerly wind anomalies in the southern part of Amazon.

In addition to the meteorological fields, we also investigated the difference in OCS surface emission between August–October (dry season) and January–March (wet season). Results are summarized in Figure 3. OCS emission differences (dry season—wet season) from vegetation uptake is positive over the Central and Southern Amazon basin and negative over the northern part of the Amazon (Figure 3a), which is consistent with the precipitation anomalies. Less precipitation over the Central and Southern Amazon basin will limit available water to the plants, resulting in reduced photosynthetic activities (see, e.g., Albright et al., 2022). As a result, less OCS is taken up by the vegetation over the Central and Southern Amazon basin during August–October (dry season) than January–March (wet season). During August–October (dry season), there is more biomass burning in the Central and Southern Amazon region (Jiang et al., 2021). Therefore, more OCS is emitted from biomass burning over the Central and Southern Amazon basin during August–October (dry season) (Figure 3b).

OCS uptake by soil can be influenced by temperature and soil moisture (Kesselmeier et al., 1999). Kesselmeier et al. (1999) found that the OCS uptake by soil decreases with temperature when temperature is higher than 20°C . We calculated the soil temperature during August–October (dry season) and January–March (wet season) in Figure S2 in Supporting Information S1. Soil temperature is always higher than 20°C in the Amazon, and it is higher during August–October (dry season) than January–March (wet season). As a response to the temperature differences, there is less OCS uptake by soil during August–October (dry season). Precipitation and soil moisture over the Central and Southern Amazon region are both lower during August–October (dry season), and these conditions will result in less removal of OCS from the atmosphere. As a result, there are positive OCS anomalies from the soil over the Central and Southern Amazon during August–October (dry season) (Figure 3c).

OCS ocean emission differences between August–October (dry season) and January–March (wet season) are shown in Figure 3d. There are negative OCS ocean emission anomalies over most regions during the dry relative to the wet season, which is consistent with results in Kettle et al. (2002). Since the magnitude of OCS ocean

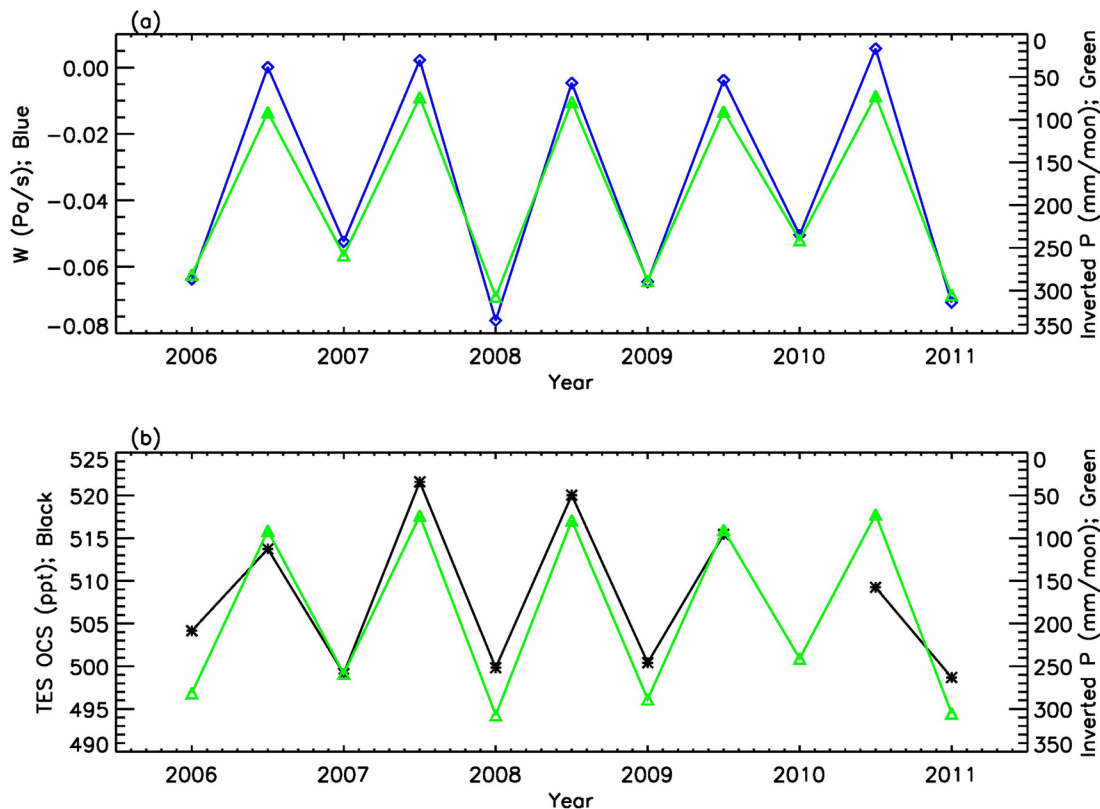


Figure 4. (a) Time series of 511 hPa vertical pressure velocity (W , blue line) and inverted Global Precipitation Climatology Project (GPCP) precipitation (P , green line). (b) Time series of Tropospheric Emission Spectrometer (TES) mid-tropospheric OCS (black line) and inverted GPCP precipitation (P , green line). Data are averaged over 288°–314°E, 20°–0°S for January–March (wet season) and August–October (dry season). Units for vertical pressure velocity, precipitation, and OCS are Pa s⁻¹, mm month⁻¹, and ppt. TES mid-tropospheric OCS are missing in January–March of 2010.

emission difference is smaller than other emissions (<10% of the OCS vegetation uptake), horizontal transport of OCS from the ocean play a minor role in the OCS anomalies over the Amazon basin.

Temporal variations of different variables (inverted GPCP precipitation, NCEP2 511 hPa vertical pressure velocity, TES mid-tropospheric OCS) over the Amazon basin (288°–314°E, 20°–0°S) are shown in Figure 4. During January–March (wet season), precipitation values are high (>250 mm month⁻¹). High precipitation will bring more water to plants and increase photosynthetic activity of plants (e.g., Albright et al., 2022), removing more OCS from the atmosphere. As a result, OCS values are low during January–March wet season (Figure 4b). During August–October (dry season), the precipitation values are low (<100 mm month⁻¹). Photosynthetic activity is also low during the dry season, so OCS concentrations are high in August–October (black line in Figure 4b). There is an anti-correlation between the precipitation and TES mid-tropospheric OCS, with a correlation coefficient of -0.91 and a significance level of 1% (estimated using a Monte Carlo method; Jiang et al., 2004). More sinking air is seen over the Amazon during August–October (dry) than January–March (wet) (blue line in Figure 4a), which can help to trap OCS in the Amazon basin. 511 hPa vertical pressure velocity is positively correlated with TES mid-tropospheric OCS with a correlation coefficient of 0.89 (1% significance level).

NCEP1 reanalysis meteorological field and OCS surface fluxes are used to drive the MOZART-4 model. Differences of MOZART-4 OCS between August–October (dry season) and January–March (wet season) at the surface and mid-troposphere are shown in Figure 5. At the surface (995 hPa), there are positive OCS anomalies over the southern part of the Amazon and negative OCS anomalies over the northern part (Figure 5a). TES mid-tropospheric averaging kernel was applied to the MOZART-4 OCS vertical profile to estimate the convolved mid-tropospheric model OCS, so it can be compared to TES mid-tropospheric OCS retrievals. In the mid-troposphere, there are positive MOZART-4 OCS anomalies over the Central and Southern Amazon, while there are negative MOZART-4 OCS anomalies over the northern part of Amazon (Figure 5b), which are similar

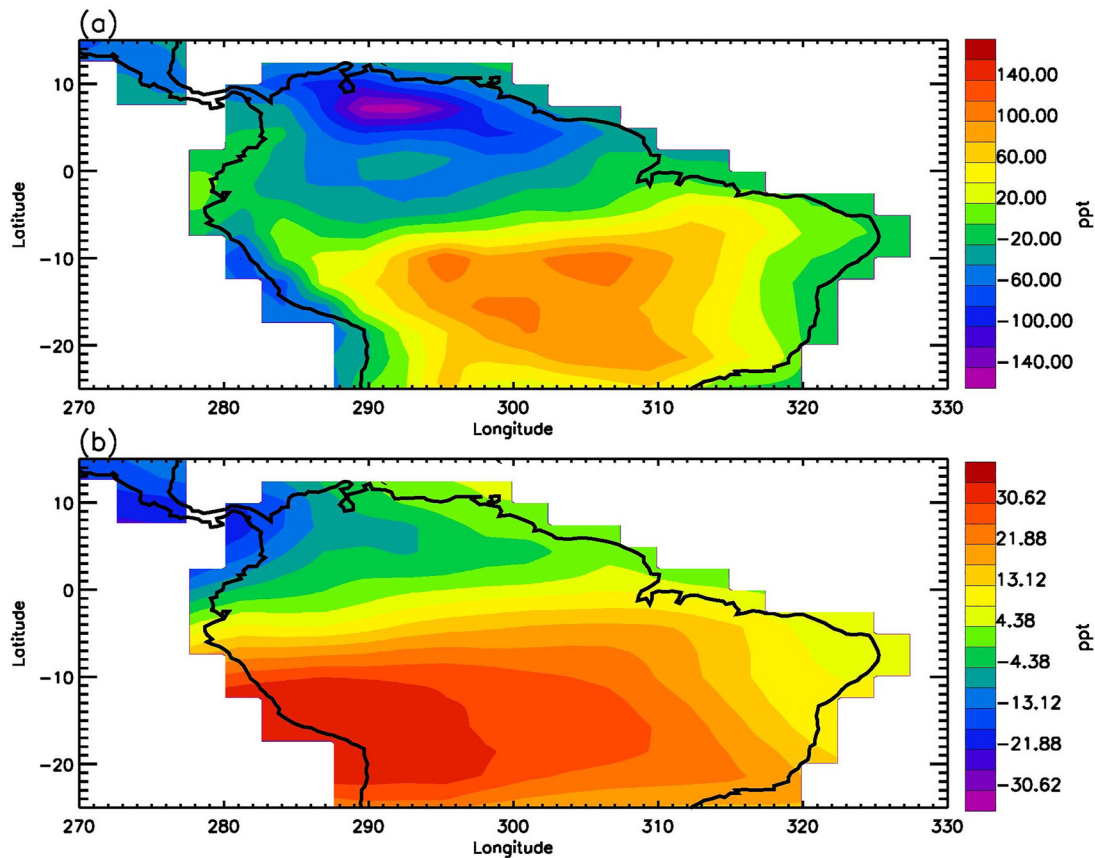


Figure 5. MOZART-4 OCS difference between August–October (dry season) and January–March (wet season) at (a) 995 hPa and (b) mid-troposphere. Units are ppt.

to those from TES mid-tropospheric OCS retrievals (Figure 1c). The MOZART-4 OCS difference between August–October (dry season) and January–March (wet season) is about 20 ppt over 288°–314°E, 20°–0°S, which is similar to the TES OCS difference (~16 ppt). The spatial distribution of OCS difference is slightly different between the MOZART-4 model OCS and TES mid-tropospheric OCS retrievals. Since the climatological OCS surface fluxes are used in the simulation, it might cause discrepancies between the MOZART-4 model OCS and TES mid-tropospheric OCS retrievals. TES OCS error is <0.6 ppt in each grid cell, which also should be considered when we compare model results to TES OCS retrievals. In the future, we can use satellite OCS data to better constrain the OCS surface emissions, especially the interannual variability.

4. Conclusions

OCS is removed from the atmosphere during the photosynthesis process; however, it is not involved in the respiration process (Brown & Bell, 1986; Campbell et al., 2008; Kettle et al., 2002; Protoschill-Krebs & Kesselmeier, 1992; Protoschill-Krebs & Wilhelm, 1996). Unlike CO₂, which is involved in both photosynthesis and respiration, OCS can be used to track photosynthetic activities from the biosphere. In this paper, we have utilized mid-tropospheric OCS retrievals from TES satellite to reveal the impact of dry/wet conditions on distributions of the mid-tropospheric OCS over the whole Amazon basin. Mid-tropospheric OCS retrievals from TES demonstrate positive OCS anomalies over the central and southern parts of the Amazon and negative OCS anomalies over the northern part of the Amazon during August–October (dry season). These results are consistent with the precipitation anomalies. During August–October (dry season), there are negative precipitation anomalies over the central and southern Amazon, which will lead to reduced photosynthetic activities. As a result, less OCS will be absorbed by vegetation, leading to a higher OCS concentration over the central and southern Amazon during the dry season. Positive precipitation anomalies are seen over the Northern Amazon, which is associated with enhanced photosynthetic activities during August–October. Thus, there are negative OCS anomalies over the northern Amazon during August–October (dry season).

We have studied meteorological conditions and OCS surface emissions during August–October (dry season) and January–March (wet season). As shown in Figure 2, there are anomalies sinking air over the Amazon during August–October, which can help to trap OCS over the basin and contribute to the positive OCS anomalies over the Central and Southern Amazon. The correlation coefficient of 511 hPa vertical pressure velocity and TES mid-tropospheric OCS is 0.89. There are more OCS emissions from the biomass burning and less OCS uptake from the vegetation and soil over the Central and Southern Amazon during August–October (dry season), which causes an increase in OCS concentrations. The difference of OCS emission from ocean is negative and relatively small; it won't have a big influence on the positive OCS anomalies over the Amazon during August–October (dry season).

MOZART-4 model is performed to simulate OCS during August–October (dry season) and January–March (wet season) and to identify sources and processes responsible for the variations of OCS concentrations in the atmosphere. MOZART-4 model shows positive OCS anomalies over the Central and Southern Amazon and negative OCS anomalies over the Northern Amazon, which is similar to the results from TES mid-tropospheric OCS. However, there are some differences in the spatial distribution of OCS in the MOZART-4 model OCS and the TES mid-tropospheric OCS retrievals.

Results from this study reveal that strengthened sinking air, less precipitation, and positive OCS surface emissions will lead to positive OCS anomalies over the Central and Southern Amazon during August–October (dry season). Although the MOZART-4 model can capture the OCS anomalies over the Amazon in the mid-troposphere, there remain differences between model and TES OCS retrievals. Satellite mid-tropospheric OCS retrievals can be used to constrain the OCS surface emissions and improve model simulations in the future.

Data Availability Statement

TES mid-tropospheric OCS data are available at <https://tes.jpl.nasa.gov/tes/data/>. Horizontal winds, vertical pressure velocity, and surface soil temperature data can be accessed at <https://psl.noaa.gov/data/gridded/data.ncep.reanalysis2.html>. The precipitation data sets can be found at <https://psl.noaa.gov/data/gridded/data.gpcp.html>.

References

- Abadie, C., Maignan, F., Remaud, M., Ogee, J., Campbell, J. E., Whelan, M. E., et al. (2022). Global modelling of soil carbonyl sulfide exchanges. *Biogeosciences*, 19(9), 2427–2463. <https://doi.org/10.5194/bg-19-2427-2022>
- Adler, R. F., Sapiano, M. R. P., Huffman, G. J., Wang, J. J., Gu, G., Bolvin, D., et al. (2018). The Global Precipitation Climatology Project (GPCP) monthly analysis (new version 2.3) and a review of 2017 global precipitation. *Atmosphere*, 9(4), 138. <https://doi.org/10.3390/atmos9040138>
- Albright, R., Corbett, A., Jiang, X., Creedy, E., Newman, S., Li, K. F., et al. (2022). Seasonal variations of solar-induced fluorescence, precipitation, and carbon dioxide over the Amazon. *Earth and Space Science*, 9(1), e2021EA002078. <https://doi.org/10.1029/2021EA002078>
- Berry, J., Wolf, A., Campbell, J. E., Baker, I., Blake, N., Blake, D., et al. (2013). A coupled model of the global cycles of carbonyl sulfide and CO₂: A possible new window on the carbon cycle. *Journal of Geophysical Research: Biogeosciences*, 118(2), 842–852. <https://doi.org/10.1002/jgrg.20068>
- Bevington, P. R., & Robinson, D. K. (2003). *Data reduction and error analysis for the physical science* (p. 336). McGraw-Hill.
- Blake, N. J., Campbell, J. E., Vay, S. A., Fuelberg, H. E., Huey, L. G., Sachse, G., et al. (2008). Carbonyl sulfide (OCS): Large-scale distributions over North America during INTEX-NA and relationship to CO₂. *Journal of Geophysical Research*, 113(D9), D09S90. <https://doi.org/10.1029/2007JD009163>
- Boone, C. D., Nassar, R., Walker, K. A., Rochon, Y., McLeod, S. D., Rinsland, C. P., & Bernath, P. F. (2005). Retrievals for the atmospheric chemistry experiment Fourier-transform spectrometer. *Applied Optics*, 44(33), 7218–7231. <https://doi.org/10.1364/ao.44.007218>
- Brown, K. A., & Bell, J. N. B. (1986). Vegetation – The missing sink in the global cycle of carbonyl sulphide (COS). *Atmospheric Environment*, 20(3), 537–540. [https://doi.org/10.1016/0004-6981\(86\)90094-6](https://doi.org/10.1016/0004-6981(86)90094-6)
- Campbell, J. E., Carmichael, G. R., Chai, T., Mena-Carrasco, M., Tang, Y., Blake, D. R., et al. (2008). Photosynthetic control of atmospheric carbonyl sulfide during the growing season. *Science*, 332(5904), 1085–1088. <https://doi.org/10.1126/science.1164015>
- Campbell, J. E., Whelan, M. E., Seibt, U., Smith, S. J., Berry, J. A., & Hilton, T. W. (2015). Atmospheric carbonyl sulfide sources from anthropogenic activity: Implications for carbon cycle constraints. *Geophysical Research Letters*, 42(8), 3004–3010. <https://doi.org/10.1002/2015gl063445>
- Chin, M., & Davis, D. D. (1993). Global sources and sinks of OCS and CS₂ and their distributions. *Global Biogeochemical Cycles*, 7(2), 321–337. <https://doi.org/10.1029/93gb00568>
- Chin, M., & Davis, D. D. (1995). A reanalysis of carbon sulfide as a source of stratosphere background sulfur aerosol. *Journal of Geophysical Research*, 100(D5), 8993–9005. <https://doi.org/10.1029/95jd00275>
- Crutzen, P. J. (1976). The possible importance of CSO for the sulphate layer of the stratosphere. *Geophysical Research Letters*, 3(2), 73–76. <https://doi.org/10.1029/gl003i002p00073>
- Emmons, L. K., Walters, S., Hess, P. G., Lamarque, J.-F., Pfister, G. G., Fillmore, D., et al. (2010). Description and evaluation of the model for ozone and related chemical tracers, version 4 (MOZART-4). *Geoscientific Model Development*, 3(1), 43–67. <https://doi.org/10.5194/gmd-3-43-2010>
- Glatthor, N., Hopfner, M., Baker, I. T., Berry, J., Campbell, J. E., Kawa, S. R., et al. (2015). Tropical sources and sinks of carbonyl sulfide observed from space. *Geophysical Research Letters*, 42(22), 10082–10090. <https://doi.org/10.1002/2015gl066293>

Acknowledgments

The authors thank two anonymous referees and the editor for their time and constructive suggestions. X. Jiang was supported by NASA ROSES NNH19ZDA001N-CDAP Program.

- Glatthor, N., Hopfner, M., Leyser, A., Stiller, G. P., von Clarmann, T., Grabowski, U., et al. (2017). Global carbonyl sulfide (OCS) measured by MIPAS/Envisat during 2002–2012. *Atmospheric Chemistry and Physics*, 17(4), 2631–2652. <https://doi.org/10.5194/acp-17-2631-2017>
- Hu, L., Montzka, S. A., Kaushik, A., Andrews, A. E., Sweeney, C., Miller, J., et al. (2021). COS-derived GPP relationships with temperature and light help explain high-latitude atmospheric CO₂ seasonal cycle amplification. *Proceedings of the National Academy of Sciences of the United States of America*, 118(33). <https://doi.org/10.1073/pnas.2103423118>
- Jiang, X., Camp, C. D., Shia, R., Noone, D., Walker, C., & Yung, Y. L. (2004). Quasi-biennial oscillation and quasi-biennial oscillation-annual beat in the tropical total column ozone: A two-dimensional model simulation. *Journal of Geophysical Research*, 109(D16), D16305. <https://doi.org/10.1029/2003JD004377>
- Jiang, X., Li, K. F., Liang, M. C., & Yung, Y. L. (2021). Impact of Amazonian fires on atmospheric CO₂. *Geophysical Research Letters*, 48(5), e2020GL091875. <https://doi.org/10.1029/2020GL091875>
- Kalnay, E., Kanamitsu, M., Kistler, R., Collins, W., Deaven, D., Gandin, L., et al. (1996). NCEP/NCAR 40-year reanalysis project. *Bulletin of the American Meteorological Society*, 77, 437–470.
- Kanamitsu, M., Ebisuzaki, W., Woollen, J., Yang, S.-K., Hnilo, J. J., Fiorino, M., & Potter, G. L. (2002). NCEP-DOE AMIP-II reanalysis (R2). *Bulletin of the American Meteorological Society*, 83(11), 1631–1643. [https://doi.org/10.1175/bams-83-11-1631\(2002\)083<1631:nar>2.3.co;2](https://doi.org/10.1175/bams-83-11-1631(2002)083<1631:nar>2.3.co;2)
- Kesselmeier, J., Teusch, N., & Kuhn, U. (1999). Controlling variables for the uptake of atmospheric carbonyl sulfide by soil. *Journal of Geophysical Research*, 104(D9), 11577–11584. <https://doi.org/10.1029/1999jd900090>
- Kettle, A. J., Kuhn, U., von Hobe, M., Kesselmeier, J., & Andreae, M. O. (2002). Global budget of atmospheric carbonyl sulfide: Temporal and spatial variations of the dominant sources and sinks. *Journal of Geophysical Research*, 107(D22), 4658. <https://doi.org/10.1029/2002JD002187>
- Ko, M. K. W., Poulet, G., Blake, D. R., Boucher, O., Burkholder, J. H., Chin, M., et al. (2003). *Very short-lived halogen and sulfur substances. Scientific assessment of Ozone depletion, global Ozone research and monitoring Project – Report No. 47*. World Meteorological Organization.
- Kooijmans, L. M. J., Cho, A., Ma, J., Kaushik, A., Haynes, K. D., Baker, I., et al. (2021). Evaluation of carbonyl sulfide biosphere exchange in the Simple Biosphere Model (SiB4). *Biogeosciences*, 18(24), 6547–6565. <https://doi.org/10.5194/bg-18-6547-2021>
- Krysztofiak, G., Te, Y. V., Catoire, V., Berthet, G., Toon, G. C., Jegou, F., et al. (2014). Carbonyl sulphide (OCS) variability with latitude in the atmosphere. *Atmosphere-Ocean*, 53, 1–13. <https://doi.org/10.1080/07055900.2013.876609>
- Kuai, L., Worden, J., Kulawik, S. S., Montzka, S. A., & Liu, J. (2014). Characterization of Aura TES carbonyl sulfide retrievals over ocean. *Atmospheric Measurement Techniques*, 7(1), 163–172. <https://doi.org/10.5194/amt-7-163-2014>
- Kuai, L., Worden, J. R., Campbell, J. E., Kulawik, S. S., Li, K. F., Lee, M., et al. (2015). Estimate of carbonyl sulfide tropical oceanic surface fluxes using Aura Tropospheric Emission Spectrometer observations. *Journal of Geophysical Research: Atmospheres*, 120(20), 11012–11023. <https://doi.org/10.1002/2015jd023493>
- Lennartz, S. T., Gauss, M., von Hobe, M., & Marandino, C. A. (2021). Monthly resolved modelled oceanic emissions of carbonyl sulphide and carbon disulphide for the period 2000–2019. *Earth System Science Data*, 13(5), 2095–2110. <https://doi.org/10.5194/essd-13-2095-2021>
- Ma, J., Kooijmans, L. M. J., Cho, A., Montzka, S. A., Glatthor, N., Worden, J. R., et al. (2021). Inverse modelling of carbonyl sulfide: Implementation, evaluation and implications for the global budget. *Atmospheric Chemistry and Physics*, 21(5), 3507–3529. <https://doi.org/10.5194/acp-21-3507-2021>
- Maignan, F., Abadie, C., Remaud, M., Kooijmans, L. M. J., Kohonen, K., Commane, R., et al. (2021). Carbonyl sulfide: Comparing a mechanistic representation of the vegetation uptake in a land surface model and the leaf relative uptake approach. *Biogeosciences*, 18(9), 2917–2955. <https://doi.org/10.5194/bg-18-2917-2021>
- Maseyk, L., Berry, J. A., Billesbach, D., Campbell, J. E., Torn, M. S., Zahniser, M., & Seibt, U. (2014). Sources and sinks of carbonyl sulfide in an agricultural field in the Southern Great Plains. *Proceedings of the National Academy of Sciences of the United States of America*, 111(25), 9064–9069. <https://doi.org/10.1073/pnas.1319132111>
- Montzka, S. A., Calvert, P., Hall, B. D., Elkins, J. W., Conway, T. J., Tans, P. P., & Sweeney, C. (2007). On the global distribution, seasonality, and budget of atmospheric carbonyl sulfide (COS) and some similarities to CO₂. *Journal of Geophysical Research*, 112(D9), D09302. <https://doi.org/10.1029/2006JD007665>
- Notholt, J., Kuang, Z., Rinsland, C. P., Toon, G. C., Rex, M., Jones, N., et al. (2003). Enhanced upper tropical tropospheric COS: Impact on the stratospheric aerosol layer. *Science*, 300(5617), 307–310. <https://doi.org/10.1126/science.1080320>
- Protoschill-Krebs, G., & Kesselmeier, J. (1992). Enzymatic pathways for the consumption of carbonyl sulphide (COS) by higher plants. *Botanica Acta*, 105(3), 206–212. <https://doi.org/10.1111/j.1438-8677.1992.tb00288.x>
- Protoschill-Krebs, G., Wilhelm, C., & Kesselmeier, J. (1996). Consumption of carbonyl sulphide (OCS) by higher plant carbonic anhydrase (CA). *Atmospheric Environment*, 30(18), 3151–3156. [https://doi.org/10.1016/1352-2310\(96\)00026-x](https://doi.org/10.1016/1352-2310(96)00026-x)
- Remaud, M., Chevallier, F., Maignan, F., Belviso, S., Berchet, A., Parouffe, A., et al. (2022). Plant gross primary production, plant respiration and carbonyl sulfide emissions over the globe inferred by atmospheric inverse modelling. *Atmospheric Chemistry and Physics*, 22(4), 2525–2552. <https://doi.org/10.5194/acp-22-2525-2022>
- Rodgers, C. D. (2000). *Inverse methods for atmospheric sounding: Theory and practice* (p. 256). World Scientific.
- Spielmann, F. M., Wohlfahrt, G., Hammerle, A., Kitz, F., Migliavacca, M., Alberti, G., et al. (2019). Gross primary productivity of four European Ecosystems constrained by joint CO₂ and COS flux measurements. *Geophysical Research Letters*, 46(10), 5284–5293. <https://doi.org/10.1029/2019gl082006>
- Stinecipher, J. R., Cameron-Smith, P., Kuai, L., Glatthor, N., Hopfner, M., Baker, I., et al. (2022). Remotely sensed carbonyl sulfide constrains model estimates of Amazon primary productivity. *Geophysical Research Letters*, 49(9), e2021GL096802. <https://doi.org/10.1029/2021GL096802>
- Stinecipher, J. R., Cameron-Smith, P. J., Blake, N. J., Kuai, L., Lejeune, B., Mahieu, E., et al. (2019). Biomass burning unlikely to account for missing source of carbonyl sulfide. *Geophysical Research Letters*, 46(24), 14912–14920. <https://doi.org/10.1029/2019gl085567>
- Thornton, D. C., Bandy, A. R., Blomquist, B. W., & Anderson, B. E. (1996). Impact of anthropogenic and biogenic sources and sinks on carbonyl sulfide in the North Pacific troposphere. *Journal of Geophysical Research*, 101(D1), 1873–1881. <https://doi.org/10.1029/95jd00617>
- Watts, S. F. (2000). The mass budgets of carbonyl sulfide, dimethyl sulfide, carbon disulfide and hydrogen sulfide. *Atmospheric Environment*, 34(5), 761–779. [https://doi.org/10.1016/s1352-2310\(99\)00342-8](https://doi.org/10.1016/s1352-2310(99)00342-8)
- Whelan, M. E., Lennartz, S. T., Gimeno, T. E., Wehr, R., Wohlfahrt, G., Wang, Y., et al. (2018). Reviews and syntheses: Carbonyl sulfide as a multi-scale tracer for carbon and water cycle. *Biogeosciences*, 15(12), 3625–3657. <https://doi.org/10.5194/bg-15-3625-2018>
- Wofsy, S. C. (2011). HIAPER Pole-to-Pole Observations (HIPPO): Fine-grained, global-scale measurements of climatically important atmospheric gases and aerosols. *Philosophical Transactions of the Royal Society A: Mathematical, Physical and Engineering Sciences*, 369(1943), 2073–2086. <https://doi.org/10.1098/rsta.2010.0313>
- Zumkehr, A., Hilton, T. W., Whelan, M., Smith, S., Kuai, L., Worden, J., & Campbell, J. E. (2018). Global gridded anthropogenic emissions inventory of carbonyl sulfide. *Atmospheric Environment*, 183, 11–19. <https://doi.org/10.1016/j.atmosenv.2018.03.063>